Available online at www.sciencedirect.com

ScienceDirect

Procedia CIRP 123 (2024) 328–333

www.elsevier.com/locate/procedia

7th CIRP Conference on Surface Integrity

Mechanics and surface characterization of high-speed diamond turning of germanium

Eann Lawing[a]*, Michele Tunesi[b], Colton Estes[c], John Gasson[c], Brian S. Dutterer[a], Don A. Lucca [b], Matthew A. Davies[a,c]

[a]*Department of Mechanical Engineering, Duke Centennial Hall, The University of North Carolina at Charlotte, Charlotte, NC, 28223*
[b] *School of Mechanical and Aerospace Engineering, 300 Engineering South, Oklahoma State Univeristy, Stillwater, OK, 74078*
[c] *Moore Nanotechnology Systems, 6510 Northpark Blvd, Charlotte, NC 28216*

* Corresponding author. Tel.: 980-422-5787; *E-mail address:* elawing4@charlotte.edu

Abstract

Germanium and other brittle single crystal materials can be diamond turned with negative rake angle tools, but to maintain surface integrity parameters are typically chosen conservatively. This work describes experiments performed on (100)Ge crystal samples that support a recent scientific finding: increasing the surface speed in diamond turning of germanium improves surface integrity. Materials are machined on a modern ultraprecision diamond turning machine at constant surface speed and constant feed per revolution keeping both the geometric character and the material flow dynamics constant during machining. Forces are measured in the experiments at cutting speeds ranging from 0.2 m/s to 10 m/s. Surface roughness of the machined surfaces was characterized using coherence scanning interferometry and surface analysis. The key findings of the work are (a) force and specific forces decrease by approximately a factor of 2 over the cutting speed range and (b) surface damage substantively decreases with cutting speed. This is correlated to the behavior of the cutting forces during machining and the chip geometry. The findings indicate that higher material removal rates can be obtained in diamond turning of germanium and that this increase in material remove rates also improves surface integrity.

© 2024 The Authors. Published by Elsevier B.V.
This is an open access article under the CC BY-NC-ND license (https://creativecommons.org/licenses/by-nc-nd/4.0)
Peer-review under responsibility of the scientific committee of the 7th CIRP Conference on Surface Integrity

Keywords: Germanium; Diamond Turning; Surface Characterization

1. Introduction

For centuries, optics have been designed using flat and spherical surfaces due to both the *relative* ease of manufacturing and measuring these surfaces. Freeform optical systems, which are defined as surfaces which have no axis of rotational invariance [1, 2], are becoming more feasible due to multi-axis ultraprecision machine tools. One growing area of application of freeform optics is infrared systems where the machining of nominally brittle materials is prevalent. These brittle materials, such as germanium and silicon, often have favorable properties for transmission of light in the infrared spectrum. Further at infrared wavelengths (approximately 1.5 μm to 12 μm) the tolerances on surface roughness and form are greater than for visible optics and this makes complex freeform surfaces with these tolerances more attainable with multi-axis diamond machining. Germanium has been prevalent in infrared optics and detectors since 1950 due to its availability of it in its single-crystalline form [3]. Both silicon and germanium have also been applied in x-ray optical systems [4]. Freeform surfaces in germanium are of particular interest to the field of freeform optics. The brittle nature of germanium and the ability

2212-8271 © 2024 The Authors. Published by Elsevier B.V.
This is an open access article under the CC BY-NC-ND license (https://creativecommons.org/licenses/by-nc-nd/4.0)
Peer-review under responsibility of the scientific committee of the 7th CIRP Conference on Surface Integrity
10.1016/j.procir.2024.05.058

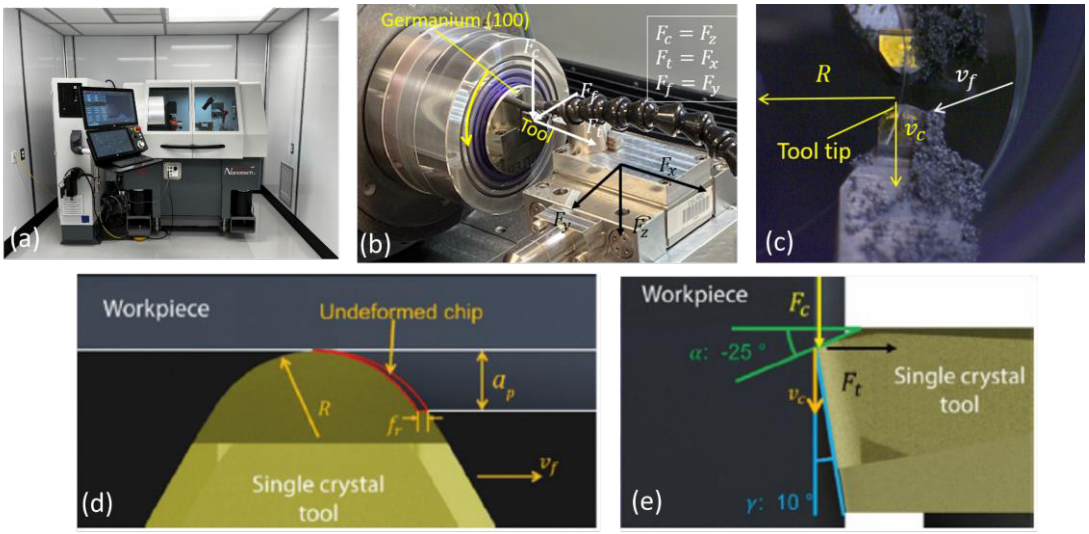

Figure 1: Setup of the experiment and important variables (a) Moore Nanotechnology 250 UPL-MP machine. (b) the sample, tool, and dynamometer on the machine (c) magnified view of the cutting process. (d) definitions of the tool radius R, the feed pre revolution f_r, the depth of cut a_p, and the feed velocity v_f (e) the thrust force F_t, the cutting force F_c, and the cutting velocity v_c

to machine it with diamond tools having a negative rake angle, which suppresses brittle fracture, makes ultra-precision machining the only viable method for producing such surfaces [5]. Since the machining of more complex surfaces means that parameters vary through the cutting, a better understanding of the cutting mechanics in diamond machining of germanium is necessary.

There is a substantial literature on the machining of germanium and other brittle materials. This machining is facilitated by producing significant hydrostatic pressure during machining with negative rake angle cutting tools. This suppresses brittle fracture and encourages shear deformation, and optical level roughness can be attained [6]. Nakasuji et. al. demonstrated shear dominated machining and also the effect of crystal orientation on the damage patterns in the surface [7]. Blackley and Scattergood showed that there is a limit for which single crystal germanium can be machined without significant surface fracture [8]. Lucca et al. studied the effects of using negative rake tools in the diamond turning of germanium to suppress fracture [9]. However, the mechanisms by which shear dominates over fracture is not well understood. Further, previous literature has focused only on the geometry of the cutting operations. The maximum chip dimension is said to control so-called "ductile regime machining". Often surface fracture does appear suddenly at some apparent "critical chip thickness" and this has led to the conclusion that there is an abrupt transition in the cutting mechanism. However, this is a misnomer, as research on the subsurface character of the machined materials indicates that subsurface damage increases continuously with the scale of the chip formation. Owen et al. and others have demonstrated that this is not the case. In the subsurface, the transition is gradual, not abrupt [10], so the idea of "ductile regime machining" is attractive but is simply not supported by careful experiments. Further, because of the focus on chip geometry, little research focuses on dynamic effects that occur due to changes in cutting speed (i.e., average strain rate, etc.). In cutting freeform optics with high-speed milling, for example, these effects become much more prominent [11, 12]. In this work, the effect of cutting speed is examined and is motivated by the high-speed milling of germanium at cutting speeds exceeding 4 m/s as shown in Owen et al. [10] and subsequent decrease in surface facture [15].

2. Experimental Arrangement

A flat single crystal (100)Ge specimen was machined using a Moore Nanotechnology 250 UPL-MP in the configuration shown in Fig. 1a and Fig. 1b. The specimen was turned using a single crystal diamond tool manufactured by K&Y Diamond with a 1.008 mm tool nose radius (R), a -25° rake angle (α), and a 10° conical clearance angle (γ). The depth of cut (a_p), the spindle speed (Ω), the cutting velocity (v_c), the feed velocity (v_f) and the feed per spindle revolution (f_r) were controlled. The tool was positioned so that the shank was perpendicular to the surface of the part.

A Kistler MicroDyn dynamometer was used to measure the forces as shown in Fig. 1b. The dynamometer signal was measured with a NI-DAQ board. A data acquisition frequency of 10 kHz was used to avoid aliasing (the bandwidth of the dynamometer is less than 5kHz).

Six 2-mm bands were machined at different values of v_c ranging from 0.2 m/s to 10 m/s, as shown in Fig. 2; these bands were machined with machining parameters of a_p = 10 µm and f_r = 4 µm/rev, as well as a constant surface speed. The coolant

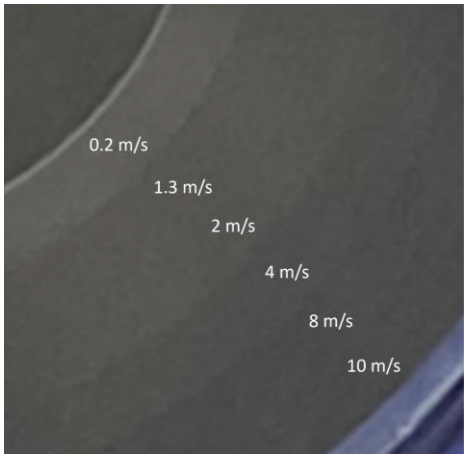

Figure 2: Bands and speeds machined during the experiment.

was a mineral spirit mist. To reduce force noise from the coolant nozzle, tests were performed to determine the lowest coolant flow rate needed to remove the chips and to match industry standards.

Before every test, several clean-up passes were performed with a_p = 10 µm, f_r = 0.3 µm/rev, and Ω = 10000 RPM. The parameters were based on work done by Sizemore [2], showing that diamond turning with these parameters was nearly as able to remove surface damage as chemo-mechanical polishing.

3. Data Analysis

3.1. Analysis Process for the Forces

The forces were processed as follows. First, the data was window-filtered to reduce noise. To keep effects of the oscillatory nature of the machining, the width of the window for the filter was made to be 1/100 of the period of the spindle. Drift was removed as demonstrated in Fig. 3. The baseline was subtracted from the measurement to eliminate the drift from the piezoelectric dynamometer. The data was trimmed, and the steady state analyzed. Mean values of cutting force ($F_{c,\,avg}$) and thrust force ($F_{t,\,avg}$) were calculated. The feed forces were also measured but were determined to be insignificant compared to the cutting and thrust force, with an approximate ratio between the thrust and feed forces of 25:1. The force magnitude and angle were calculated from F_t and F_c using Eqns. 1 and 2.

$$|F| = \sqrt{F_t + F_c} \tag{1}$$

$$\theta = \arctan\left(\frac{F_t}{F_c}\right) \tag{2}$$

The average, maximum value and minimum value were then calculated for the force magnitude and force angle. The cutting energy K_c and thrust force coefficient K_t were calculated from the average cutting force and thrust force, $F_{c,\,avg}$ and $F_{t,\,avg}$ respectively, with Eqn. 3 and Eqn. 4.

$$K_c = \frac{F_{c,avg}}{a_p f_r} \tag{3}$$

$$K_t = \frac{F_{t,avg}}{a_p f_r} \tag{4}$$

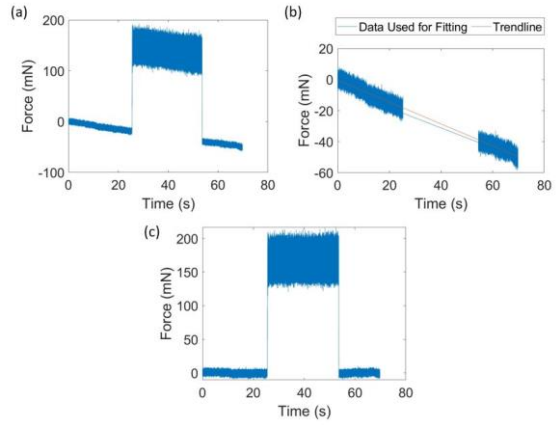

Figure 3: Example process for eliminating the drift from the data. (a) Raw data (after trimmed of excess data and window-filtered). (b) Demonstration of the creation of the trendline using the points before and after touch-off. (c) Data after the trendline has been removed.

Figure 4: Zygo ZeGage used for measurement of the surface of the sample during the experiment.

3.2. Analysis Process for the Surface Measurements

Measurements of the surface were taken using a Zygo ZeGage White Light Interferometer (Fig. 4). A 50x objective with numerical aperture (NA) of 0.55 was programmed for a stitching process that measured the from the inner most band boundary at radius R = 13 mm to the outer boundary at R = 25 mm. The number of measurements, N, needed to measure a length of material, L, for a single row of stitching was calculated using Eqn. 5.

$$N = \left\lceil \frac{L - L_{FOV}}{L_{FOV}(1-k)} \right\rceil + 1 \tag{5}$$

where L_{FOV} is the side length of the field of view, and k = 0.2 is the percentage of overlap between any two measurements.

A rotating platform was used to determine the measurement angle. The germanium sample was oriented on the platform so that the center of one of the primary damage lobes was at 0°. The angle range was 0° to 90° with 5° increments.

The Mx software was used to analyze the data. A plane form was removed from the raw surface data. Then, a band-pass FFT filter with limits of 1 µm to 25 µm was applied to the surface data. Standard roughness parameters were calculated. The surface roughness parameters were then extracted, and the above process was repeated for all the measurements. Measurements containing edges of bands were removed and the locations were correlated to cutting speeds. Outliers were removed and average parameters were calculated for each cutting speed.

3.3. Choice of Surface Roughness Parameters

Several ISO parameters were examined and correlated to damage. The parameters that are shown in this work are S_a and S_q, the pit density parameter S_{vd}, and the dale void volume parameter V_{vv}. These are defined in ISO Standard 25178-2. S_a and S_q were chosen as the industry standards. The pit density, S_{vd}, was calculated indirectly through determination of the number of dales in the measurement and dividing by the measurement area. Determination of the number of dales was

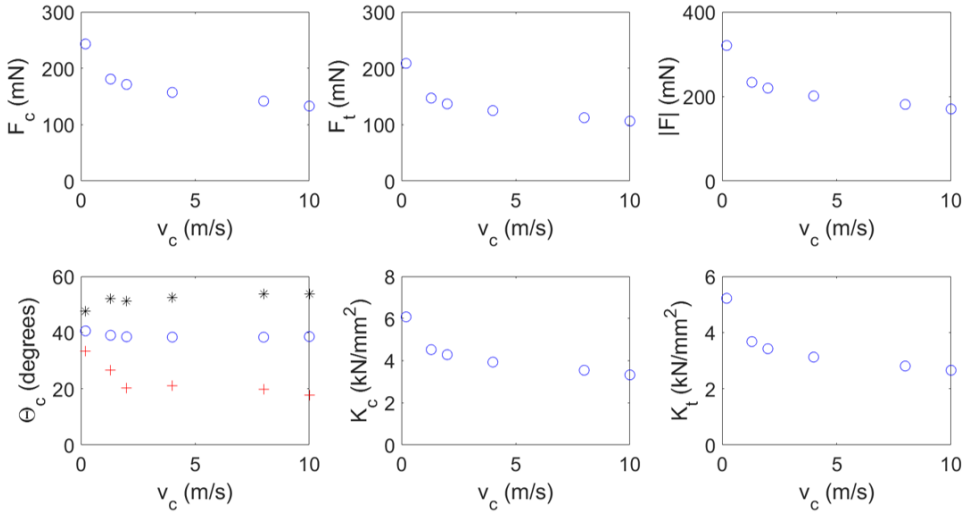

Figure 5: Analysis of the force test data. For the cutting angle (Θ_c), the red points represents the minimum value, the blue points represent the average value and the black points represent the maximum value;

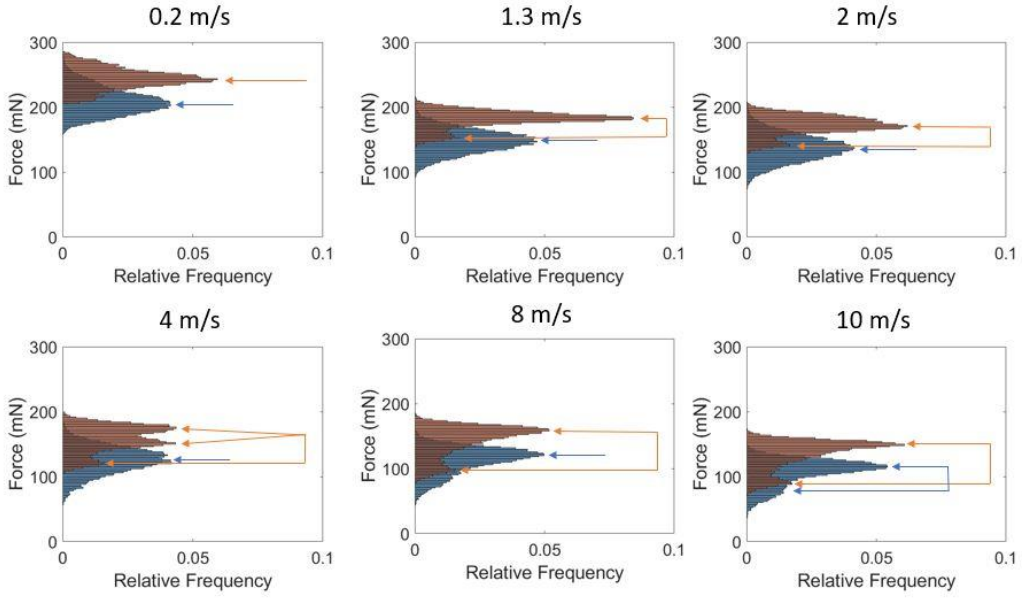

Figure 6: Histograms of the force data for different cutting speeds. The orange bars represent F_c and the blue bars represent the thrust force F_t. As the speed increases, the distributions gain a more prominent secondary peak. The orange and blue arrows indicate local maximum and potential additional peaks in the distribution.

done through watershed analysis in the Mx software with a wolf-pruning parameter of 5.0% of the value of S_z.

The dale void volume parameter was defined using the ISO standard as the amount of volume per unit area of void area from the lowest depth of the surface to a secondary depth, which is the depth at which 20% of the material that is measurable from the surface data is at that depth or lower.

4. Results and Discussion

4.1. Force Measurements

Figure 5 shows the results of the analysis of the force data as described in Section 3.1. The data shows that as the cutting speed (v_c) increases both the cutting force and the thrust force decrease, which in turn causes the force magnitude to decrease as the cutting speed increases.

The average force angle had changed only slightly, with a range of only 38° to 40°. The difference between the maximum and minimum force angle, however, seemed to increase as the speed increased. More experiments are needed to confirm if the result is consistent.

Both the cutting energy and the thrust force coefficient decrease as the cutting speed increases.

Figure 6 shows histograms of the data collected from the first two seconds (N = 20000) after the touch-off for all the data samples. The histograms show that as the cutting speed increases, the spread of the data increases. The histogram of the data also shows that as the speed increases, the force distributions develop a secondary peak, with the appearance of the secondary peak of the cutting force being more prominent

than for the thrust force. The changes in the mean, spread, and distribution of the data at the different speeds might suggest that the germanium reacts differently to being machined at different cutting speeds.

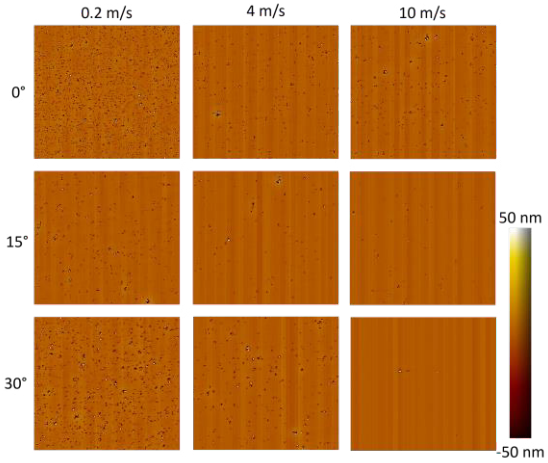

Figure 7: Results of surface white light measurements of the germanium sample showing the surface at different cutting speeds and for different angles. The angle 0° is the primary damage lobe, the secondary damage lobe is at 30°, and the region between at 15°.

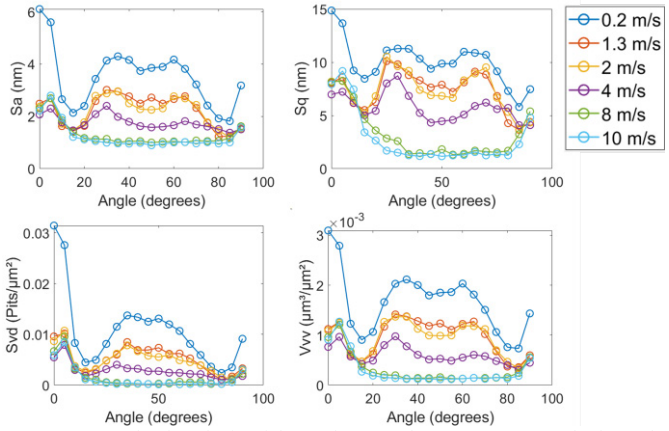

Figure 8: Result of analysis of the surface roughness parameters, the legend on the top right indicates the color associated with each speed.

4.2. Surface Measurements

Figure 7 shows some of the measurements taken of the surface for three of the bands and three of the angles using the white light interferometer. The measurements showed that areas located near primary and secondary lobes tended to have more damage than in other areas of the sample. The images taken of the surface also showed that areas that were in bands that were machined at higher cutting speeds tended to contain less evidence of surface damage than those that were in bands that were machined with lower cutting speeds.

Figure 8 shows the results of the analysis for the roughness parameters. The data from the parameters agreed with the qualitative analysis from the white light interferometry observations, with most parameters showing signs of a primary lobe at an angle near 0°, and with the band machined at 0.2 m/s seeming to have significantly higher values for nearly all the parameters. The graphs also showed that at lower cutting speeds the surface of the sample was rougher, there were more noticeable pits appeared on the surface per unit area, and there was more volume that was lost due to pits per unit area. All these factors tend to increase the power loss from reflection and refraction for most materials and thus the results showed that the bands machined at the lower cutting speeds would possibly have worse optical performance than the bands machined at higher cutting speeds.

5. Conclusion

The results from both the force data and the surface measurements seemed to contain some surprising results. The measured force data possibly indicated that at higher speeds, both the cutting force and the thrust force decrease. However, the results from surface measurements possibly showed that as the cutting speed increases, the surface of the sample has less surface damage. Although this result for germanium was documented in other research work, this is still a surprising result overall as it would be expected that the forces would be lower for a more fractured surface due to some of the forces used for cutting having to be expended to create the surface damage.

However, the change in the distribution of the data for different speeds seemed to indicate a change in cutting mechanics with speed. The change in the cutting energy and thrust force supports this theory. At present this is an experimental observation validated in other experiments by the authors [5, 10]. The reason is not known, but possible explanations include a dependency of flow stress on strain rate in germanium and thermal softening as seen in metals. A potential cause is a phase change; for example, it is known that germanium undergoes a a phase change from a crystalline phase to a beta tin (metallic) phase under high hydrostatic stress, but the effect of strain rate is not known.

However, more experiments are needed to fully understand the properties of single crystal germanium when it undergoes fracture. For instance, one aspect that was not explored in this work is how the chip morphology changes in response to different cutting speeds. These aspects will be more fully explored in future experiments.

Acknowledgements

The support of this research by NSF grants CMMI-2210365 and CMMI-2210394 is gratefully acknowledged.

References

[1] Rolland, J. P., Davies, M. A., Suleski, T. J.. Evans, C., Bauer, A., Lambropoulos, J. C. & Falaggis, K. (2021). Freeform optics for imaging. Optica, 8(2), 161-176

[2] Fang, F. Z., Zhang, X. D., Weckenmann. A., Zhang, G. X., & Evans, C., (2013). Manufacturing and measurement of freeform optics. CIRP Annals, 62(2), 823-846.

[3] Bosi, M., & Attolini, G. (2010). Germanium: Epitaxy and its applications. Progress in Crystal Growth and Characterization of Materials, 56 (3-4), 146-174.

[4] Zaprazny, Z., Korytar, D., Jergel, M., Halahovets, Y., Mat'ko, I., Siffalovic, P., Keckes, J., Mikulik, P., Majkova, E., & Tran Thi, T. N. (2019). Study of surface quality and subsurface damage of germanium optics produced by single point diamond nanomachining. SPIE Proceedings, 11032, 33-34.

[5] Sizemore, N.E. (2020). Surface Intergrity in Diamond Machining for Infrared Optics. (Doctoral dissertation, The University of North Carolina at Charlotte).
[6] Liu, K., Li, X., & Liang, S. (2007). The mechanism of ductile chip formation in cutting of brittle materials. The International Journal of Advanced Manufacturing, 33 (9-10), 875-884.
[7] Nakasuji, T., Kodera, S., Hara, S., Matsunaga, H., Ikawa, N., & Shimada, S. (1990). Diamond turning of brittle materials for optical components. CIRP Annals, 39(1), 89-92.
[8] Blackley, W. S. and Scattergood, R. O. (1990). Crystal orientation dependence of machining damage – a stress model. Journal of the American Ceramic Society, 73 (4), 949-957.
[9] Lucca, D. A., Chou, P., & Hocken, R. J. (1998). Effect of tool edge geometry on the nanometric cutting of Ge. CIRP Annals, 47(1), 475-478.
[10] Owen, J. D., Troutman, J. R., Harriman, T. A., Zare, A., Wang, Y. Q., Lucca, D. A., Davies, M. A. (2016). The mechanics of milling of germanium for IR applications. CIRP Annals, 65(1), 109-112.
[11] Zare, A., Tunesi, M., Harriman, T. A., Troutman, J. R., Davies, M. A., Lucca, D. A. (2023). Face Turning of Single Crystal (111)Ge: Cutting Mechanics and Surface/Subsurface Characteristics. J. Manuf. Sci. Eng., 145(7): 071007, 1-10.
[12] Sizemore, N. E., Nogueira, M. L., Greis, N. P., Davies, M. A. (2022). Application of machine learning for improved surface quality classification in ultra-precision machining of germanium. Journal of Manufacturing Systems, 65(1), 296-316.